

Ferromagnetic films with three to twenty spin layers as described using second order perturbed Heisenberg Hamiltonian

P. Samarasekara and T.H.Y.I.K. de Silva

Department of Physics, University of Peradeniya, Peradeniya, Sri Lanka

Abstract

Modified second order perturbed Heisenberg Hamiltonian was employed to describe the magnetic properties of ferromagnetic films with three to twenty spin layers for the first time. Previously, the solution of second order perturbed Heisenberg Hamiltonian was found for ferromagnetic films with two to five layers under some assumptions by us. In this report, the exact solution is presented without any assumptions by calculating the pseudo inverse of matrix C . All eight magnetic parameters such as spin exchange interaction, second order magnetic anisotropy, fourth order magnetic anisotropy, stress induced magnetic anisotropy, demagnetization factor, in plane magnetic field, out of plane magnetic field and magnetic dipole interaction were taken into account. The easy and hard directions were found using 3-D and 2-D plots of total magnetic energy versus these magnetic parameters. Angle between easy and hard directions was nearly 107 degrees in many cases. The magnetic easy axis gradually rotates from out of plane to in plane direction by indicating a preferred in plane orientation of magnetic easy axis for films with higher number of spin layers. These theoretical results agree with some experimental research data of ferromagnetic thin films.

Keywords: Second order perturbation, Heisenberg Hamiltonian, ferromagnetic thin films

1. Introduction:

Ferromagnetic thin films find potential applications in magnetic memory and microwave devices due to their unique properties. In compact devices, ferromagnetic thin films replace the bulk ferromagnetic materials. However, a systematic detailed theoretical study of ferromagnetic ultra thin films is not available. Classical, semi classical and quantum theoretical models are employed to describe the ferromagnetic films. While the magnitude of spin continuously varies from 0 to 1 in classical models, the spin has some discrete values in quantum models.

Ferromagnetic thin films have been studied using the Heisenberg Hamiltonian with spin exchange interaction, magnetic dipole interaction, applied magnetic field, second and fourth order magnetic anisotropy terms [1, 2, 3]. Domain structure and Magnetization reversal in thin magnetic films have been theoretically investigated [4]. In-plane dipole coupling anisotropy of a square ferromagnetic Heisenberg monolayer has been explained using Heisenberg Hamiltonian [5]. Effect of the interfacial coupling on the magnetic ordering in ferro-antiferromagnetic bilayers has been studied using the Heisenberg Hamiltonian [6].

In addition, EuTe films with surface elastic stresses have been theoretically studied using Heisenberg Hamiltonian [7]. Magnetostriction of dc magnetron sputtered FeTaN thin films has been theoretically studied using the theory of De Vries [8]. Magnetic layers of Ni on Cu have been theoretically investigated using the Korringa-Kohn-Rostoker Green's function method [9]. Electric and magnetic properties of multiferroic thin films have been theoretically explained by modified Heisenberg and transverse Ising model using Green's function technique [10]. The quasistatic magnetic hysteresis of ferromagnetic thin films grown on a vicinal substrate has been theoretically investigated by Monte Carlo simulations within a 2D model [11]. Structural and magnetic properties of two dimensional FeCo ordered alloys deposited on W(110) substrates have been studied using first principles band structure theory [12].

Previously nickel ferrite films were synthesized using sputtering by us [13]. In addition, lithium mixed ferrite films were fabricated using pulsed laser deposition [14]. For all these films, the coercivity of film increased due to the stress induced anisotropy. The change of coercivity due to the stress induced anisotropy was qualitatively calculated for all these films. The calculated values of the change of coercivity agreed with the experimentally found values. So the stress induced anisotropy plays a major role in magnetic thin fabrications. Previously the Heisenberg Hamiltonian was employed to investigate the second order perturbed energy of ultrathin ferromagnetic films [15], unperturbed energy of thick ferromagnetic films [16], third order perturbed energy of thick spinel ferrite [17], third order perturbed energy of thin spinel ferrite [18], second order perturbed energy of thick spinel ferrite films [19], spin reorientation of barium ferrite [20], third order perturbed energy of ultra-thin ferromagnetic films [21], second order perturbed energy of ferrite thin films [22] and spin reorientation of nickel ferrite films [23]. The

magnetic dipole interaction and demagnetization factor are microscopic and macroscopic effects, respectively. Therefore, both these terms were taken into consideration in our model.

2. Model:

The Heisenberg Hamiltonian of ferromagnetic films is given as following.

$$H = -\frac{J}{2} \sum_{m,n} \vec{S}_m \cdot \vec{S}_n + \frac{\omega}{2} \sum_{m \neq n} \left(\frac{\vec{S}_m \cdot \vec{S}_n}{r_{mn}^3} - \frac{3(\vec{S}_m \cdot \vec{r}_{mn})(\vec{r}_{mn} \cdot \vec{S}_n)}{r_{mn}^5} \right) - \sum_m D_{\lambda_m}^{(2)} (S_m^z)^2 - \sum_m D_{\lambda_m}^{(4)} (S_m^z)^4 \\ - \sum_{m,n} [\vec{H} - (N_d \vec{S}_n / \mu_0)] \cdot \vec{S}_m - \sum_m K_s \sin 2\theta_m$$

Here \vec{S}_m and \vec{S}_n are two spins. Above equation can be deduced to following form.

$$E(\theta) = -\frac{1}{2} \sum_{m,n=1}^N [(JZ_{|m-n|} - \frac{\omega}{4} \Phi_{|m-n|}) \cos(\theta_m - \theta_n) - \frac{3\omega}{4} \Phi_{|m-n|} \cos(\theta_m + \theta_n)] \\ - \sum_{m=1}^N (D_m^{(2)} \cos^2 \theta_m + D_m^{(4)} \cos^4 \theta_m + H_{in} \sin \theta_m + H_{out} \cos \theta_m) \\ + \sum_{m,n=1}^N \frac{N_d}{\mu_0} \cos(\theta_m - \theta_n) - K_s \sum_{m=1}^N \sin 2\theta_m \quad (1)$$

Where $J, Z_{|m-n|}, \omega, \Phi_{|m-n|}, \theta, D_m^{(2)}, D_m^{(4)}, H_{in}, H_{out}, N_d, K_s, m, n$ and N are spin exchange interaction, number of nearest spin neighbors, strength of long range dipole interaction, constants for partial summation of dipole interaction, azimuthal angle of spin, second and fourth order anisotropy constants, in plane and out of plane applied magnetic fields, demagnetization factor, stress induced anisotropy constant, spin plane indices and total number of layers in film, respectively.

In terms of small perturbations ε_m and ε_n , the azimuthal angles of spins can be expressed as $\theta_m = \theta + \varepsilon_m$ and $\theta_n = \theta + \varepsilon_n$. After substituting these new angles in above equation number 1, the cosine and sine terms can be expanded up to the second order of ε_m and ε_n as following.

$$E(\theta) = E_0 + E(\varepsilon) + E(\varepsilon^2) \quad (2)$$

$$\begin{aligned} \text{Here } E_0 = & -\frac{1}{2} \sum_{m,n=1}^N (JZ_{|m-n|} - \frac{\omega}{4} \Phi_{|m-n|}) + \frac{3\omega}{8} \cos 2\theta \sum_{m,n=1}^N \Phi_{|m-n|} \\ & - \cos^2 \theta \sum_{m=1}^N D_m^{(2)} - \cos^4 \theta \sum_{m=1}^N D_m^{(4)} - N(H_{in} \sin \theta + H_{out} \cos \theta - \frac{N_d}{\mu_0} + K_s \sin 2\theta) \quad (3) \end{aligned}$$

$$\begin{aligned} E(\varepsilon) = & -\frac{3\omega}{8} \sin 2\theta \sum_{m,n=1}^N \Phi_{|m-n|} (\varepsilon_m + \varepsilon_n) + \sin 2\theta \sum_{m=1}^N D_m^{(2)} \varepsilon_m + 2 \cos^2 \theta \sin 2\theta \sum_{m=1}^N D_m^{(4)} \varepsilon_m \\ & - H_{in} \cos \theta \sum_{m=1}^N \varepsilon_m + H_{out} \sin \theta \sum_{m=1}^N \varepsilon_m - 2K_s \cos 2\theta \sum_{m=1}^N \varepsilon_m \end{aligned}$$

$$\begin{aligned} E(\varepsilon^2) = & \frac{1}{4} \sum_{m,n=1}^N (JZ_{|m-n|} - \frac{\omega}{4} \Phi_{|m-n|}) (\varepsilon_m - \varepsilon_n)^2 - \frac{3\omega}{16} \cos 2\theta \sum_{m,n=1}^N \Phi_{|m-n|} (\varepsilon_m + \varepsilon_n)^2 \\ & - (\sin^2 \theta - \cos^2 \theta) \sum_{m=1}^N D_m^{(2)} \varepsilon_m^2 + 2 \cos^2 \theta (\cos^2 \theta - 3 \sin^2 \theta) \sum_{m=1}^N D_m^{(4)} \varepsilon_m^2 \\ & + \frac{H_{in}}{2} \sin \theta \sum_{m=1}^N \varepsilon_m^2 + \frac{H_{out}}{2} \cos \theta \sum_{m=1}^N \varepsilon_m^2 - \frac{N_d}{2\mu_0} \sum_{m,n=1}^N (\varepsilon_m - \varepsilon_n)^2 \\ & + 2K_s \sin 2\theta \sum_{m=1}^N \varepsilon_m^2 \end{aligned}$$

$$\text{After using the constraint } \sum_{m=1}^N \varepsilon_m = 0, E(\varepsilon) = \vec{\alpha} \cdot \vec{\varepsilon}$$

Here $\vec{\alpha}(\varepsilon) = \vec{B}(\theta) \sin 2\theta$ are the terms of matrices with

$$B_\lambda(\theta) = -\frac{3\omega}{4} \sum_{m=1}^N \Phi_{|\lambda-m|} + D_\lambda^{(2)} + 2D_\lambda^{(4)} \cos^2 \theta \quad (4)$$

$$\text{Also } E(\varepsilon^2) = \frac{1}{2} \vec{\varepsilon} \cdot C \cdot \vec{\varepsilon}$$

Here the elements of matrix are given by,

$$\begin{aligned}
C_{mn} = & -(JZ_{|m-n|} - \frac{\omega}{4}\Phi_{|m-n|}) - \frac{3\omega}{4}\cos 2\theta\Phi_{|m-n|} + \frac{2N_d}{\mu_0} \\
& + \delta_{mn} \left\{ \sum_{\lambda=1}^N [JZ_{|m-\lambda|} - \Phi_{|m-\lambda|} (\frac{\omega}{4} + \frac{3\omega}{4}\cos 2\theta)] - 2(\sin^2 \theta - \cos^2 \theta) D_m^{(2)} \right. \\
& \left. + 4\cos^2 \theta (\cos^2 \theta - 3\sin^2 \theta) D_m^{(4)} + H_{in} \sin \theta + H_{out} \cos \theta - \frac{4N_d}{\mu_0} + 4K_s \sin 2\theta \right\} \quad (5)
\end{aligned}$$

Therefore, the total magnetic energy given in equation 2 can be deduced to

$$E(\theta) = E_0 + \vec{\alpha} \cdot \vec{\mathcal{E}} + \frac{1}{2} \vec{\mathcal{E}} \cdot C \cdot \vec{\mathcal{E}} = E_0 - \frac{1}{2} \vec{\alpha} \cdot C^+ \cdot \vec{\alpha} \quad (6)$$

Here C^+ is the pseudo-inverse given by

$$C \cdot C^+ = 1 - \frac{E}{N}. \quad (7)$$

Here E is the matrix with all elements $E_{mn}=1$.

3. Results and Discussion:

First matrix elements of C were found using equation 5. Then elements of C^+ were determined using equation 7 and MATLAB computer program. Finally total energy was found using equation 6. When one magnetic parameter was varied, other parameters were kept at constant values. Figure 1 shows the 3-D plot of $\frac{E(\theta)}{\omega}$ versus $\frac{D_m^{(4)}}{\omega}$ and angle for ferromagnetic thin films with simple cubic (s. c.) lattice. All the graphs in figure 1 to figure 4 are given for ferromagnetic films with 3 spin layers ($N=3$). Other parameters were kept at constant values as following.

$$\frac{J}{\omega} = \frac{D_m^{(2)}}{\omega} = \frac{K_s}{\omega} = \frac{N_d}{\mu_0 \omega} = \frac{H_{in}}{\omega} = \frac{H_{out}}{\omega} = 10$$

For s. c. (001) lattice, $Z_0=4$, $Z_I=1$, $\Phi_0=9.0336$ and $\Phi_I=-0.3275$ [1, 2, 3].

Several energy maximums and minimums can be observed in this 3-D plot. One energy minimum and maximum of this 3-D plot can be found at $\frac{D_m^{(4)}}{\omega}=35$ and 25, respectively.

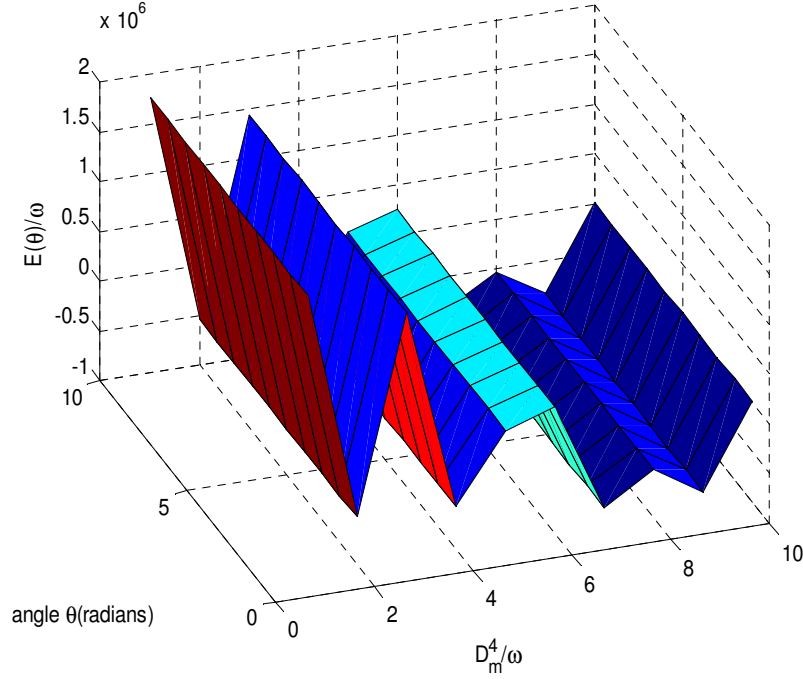


Figure 1: 3-D plot of $\frac{E(\theta)}{\omega}$ versus $\frac{D_m^{(4)}}{\omega}$ and angle for s. c. lattice

Figure 2 shows the graph of $\frac{E(\theta)}{\omega}$ versus angle at $\frac{D_m^{(4)}}{\omega}=35$. A minimum and a maximum of this plot can be observed at $10^\circ 54'$ and $123^\circ 28'$, respectively. Minimum and maximum of energy correspond to the magnetic easy and hard directions.

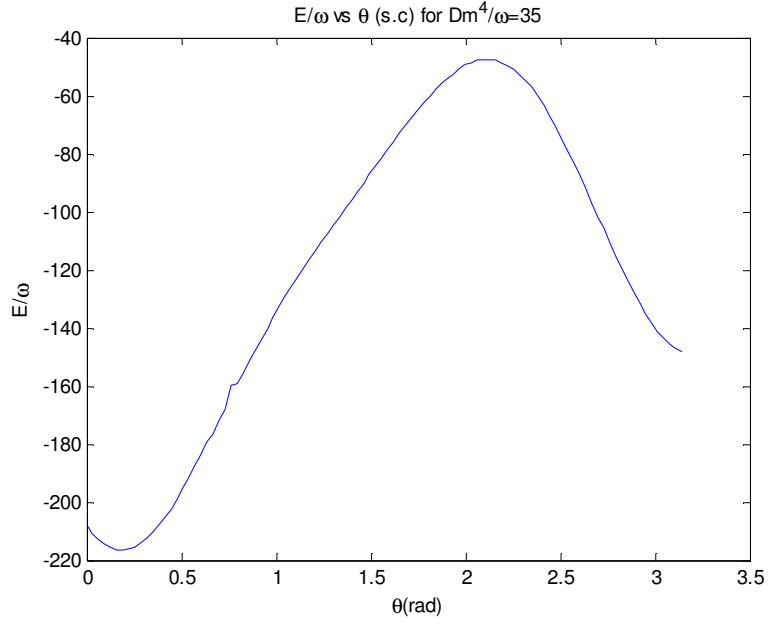


Figure 2: Graph of $\frac{E(\theta)}{\omega}$ versus angle at $\frac{D_m^{(4)}}{\omega}=35$.

Figure 3 shows the graph of $\frac{E(\theta)}{\omega}$ versus angle at $\frac{D_m^{(4)}}{\omega}=25$. A minimum and a maximum of this plot can be observed at $12^\circ 42'$ and $123^\circ 38'$, respectively. According to Figure 2 and 3, real easy and hard directions can be observed at $10^\circ 54'$ and $123^\circ 38'$, respectively.

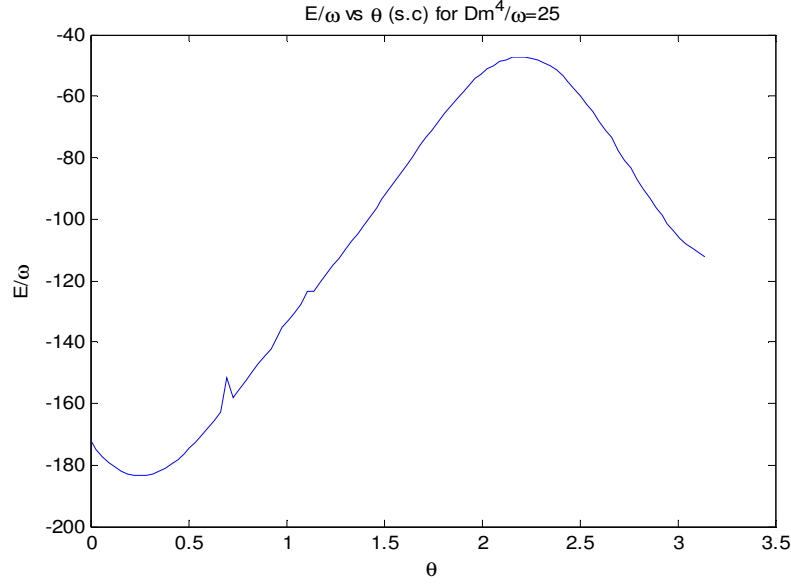


Figure 3: Graph of $\frac{E(\theta)}{\omega}$ versus angle at $\frac{D_m^{(4)}}{\omega}=25$

Figure 4 shows the 3-D plot of $\frac{E(\theta)}{\omega}$ versus angle and $\frac{D_m^{(2)}}{\omega}$. Other magnetic parameters were kept at $\frac{J}{\omega} = \frac{D_m^{(4)}}{\omega} = \frac{K_s}{\omega} = \frac{N_d}{\mu_o \omega} = \frac{H_{in}}{\omega} = \frac{H_{out}}{\omega} = 10$. Several energy maximums and minimums appear in this 3-D plot. The shape of this 3-D plot is different from the 3-D plot given in figure 1. One energy minimum and maximum can be observed at $\frac{D_m^{(2)}}{\omega}=58$ and 65, respectively. The real easy direction was found to be $10^\circ 54'$ from the graph of $\frac{E(\theta)}{\omega}$ versus angle plotted for $\frac{D_m^{(2)}}{\omega}=58$. Similarly, the real hard direction was found to be $103^\circ 38'$ from the graph of $\frac{E(\theta)}{\omega}$ versus angle plotted for $\frac{D_m^{(2)}}{\omega}=65$. All the data in this manuscript are given for s. c. structure.

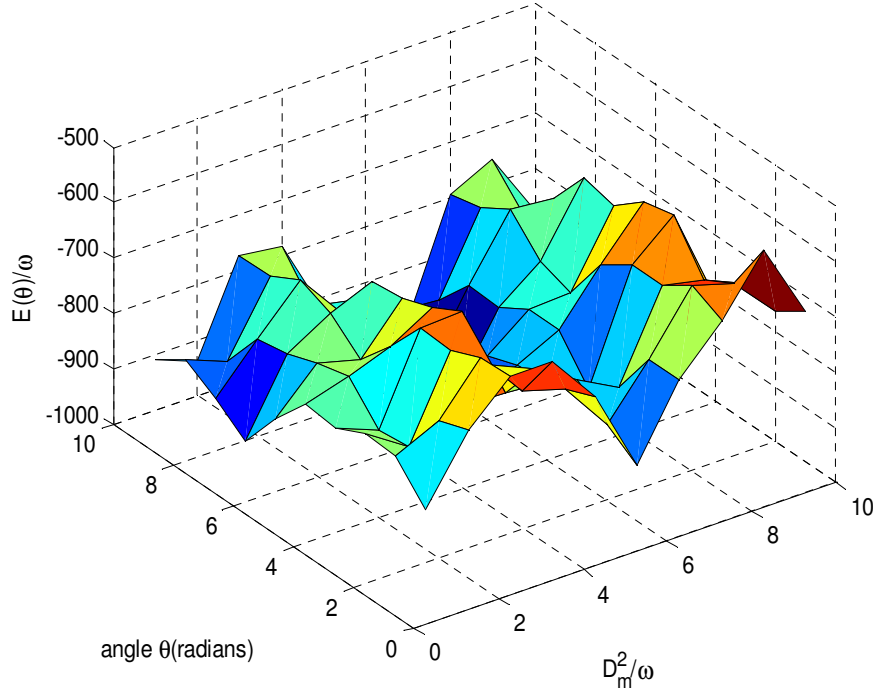


Figure 4: 3-D plot of $\frac{E(\theta)}{\omega}$ versus angle and $\frac{D_m^{(2)}}{\omega}$.

Similarly easy and hard directions were calculated for ferromagnetic films with s. c. structure using plots of $\frac{E(\theta)}{\omega}$ versus angle for $\frac{J}{\omega} = \frac{D_m^{(4)}}{\omega} = \frac{K_s}{\omega} = \frac{N_d}{\mu_o \omega} = \frac{H_{in}}{\omega} = \frac{H_{out}}{\omega} = \frac{D_m^{(2)}}{\omega} 10$ and each value of number of layers. These data are given in table 1. Columns 3, 5, 6 and 7 represent the $\frac{E(\theta)}{\omega}$ of easy direction, $\frac{E(\theta)}{\omega}$ of hard direction, energy difference between easy and hard directions and angle between easy and hard directions, respectively. Column 6 shows the energy required to rotate spins or magnetic moments from easy direction to hard direction (ΔE). In applications, materials with less ΔE are preferred. The energy required to rotate spins or magnetic moments from easy direction to hard direction gradually increases with number of layers. The angles between easy and hard directions are close to 107 degrees. Here θ is the angle between a normal drawn to film plane and the spin. Magnetic easy direction gradually rotates from out of plane to in plane direction with increase of number of layers.

These data agree with the experimental data obtained for some ferromagnetic thin films. The magnetic easy axis of sputter synthesized ferromagnetic Ni films with lattice parameter 0.352 nm indicates a preferred in plane orientation at higher thicknesses [24]. According to this experimental data, the spin reorientation transition occurs from in plane to out plane at film thickness in between 14 and 24 \AA . The magnetic easy axis of ferromagnetic Fe thin films deposited by electron beam evaporation also rotates from out of plane to in plane direction at the film thickness of 2 monolayers, as the film thickness is increased [25]. Deposition temperature, annealing temperature, orientation of substrate, type of sputtering gas, sputtering pressure, deposition rate and film thickness govern the orientation of easy axis of thin films [13, 14]. Previously, the variation of easy axis orientation of magnetic thin films with temperature has been explained by us [20, 23]. Magnetic energy due to spin exchange interaction, second order magnetic anisotropy, fourth order magnetic anisotropy, magnetic field, stress induced anisotropy decreases with the number of layers. On the other hand, magnetic energy due to magnetic dipole interaction and demagnetization factor increases with number of layers. The reason for in plane orientation of easy axis is attributed to the domination of energy due to magnetic dipole interaction and demagnetization factor at higher thicknesses.

N (Number of spin layers)	θ(easy) In degrees	E/ω (easy)	θ(hard) In degrees	E/ω (hard)	$\Delta E = E(\text{easy}) - E(\text{hard})$	$\Delta\theta = \theta(\text{hard}) - \theta(\text{easy})$ In degrees
3	27.1237	-148.4703	136.3637	-39.2801	109.1902	109.2431
4	27.2727	-201.3010	136.3638	-55.7303	145.5711	109.0911
5	32.72735	-243.2938	138.1802	-65.5296	177.7642	105.4529
6	32.72735	-293.0313	140.0022	-80.3742	212.6571	107.2749
7	32.72735	-342.4569	140.0022	-94.9925	247.4644	107.2749
8	34.54363	-391.6847	141.8185	-109.4450	282.2397	107.2749
9	34.54363	-440.6979	141.8185	-123.5873	317.1106	107.2749
10	36.36563	-489.9321	143.6348	-136.9551	352.977	107.2692
11	36.36563	-538.2348	143.6348	-151.1074	387.1274	107.2692
12	38.18191	-586.7906	145.4568	-164.3518	422.4388	107.2749
13	38.18191	-635.3465	145.4568	-177.2214	458.1251	107.2749
14	39.99818	-683.8709	147.2731	-189.5887	494.2822	107.2749
15	39.99818	-732.5906	147.2731	-201.3705	531.2201	107.2749
16	41.82019	-781.2445	149.0893	-212.7722	568.4723	107.2692
17	41.82019	-829.7926	149.0893	-233.9804	595.8122	107.2692
18	43.63647	-878.5634	150.9114	-234.6233	643.9401	107.2749
19	43.63647	-927.5520	156.3659	-243.7946	683.7574	112.7294
20	45.45274	-977.3222	152.7276	-253.1361	724.1861	107.2749

Table 1: Magnetic easy and hard directions for s. c. structured ferromagnetic films

4. Conclusion:

The magnetic properties of s. c. structured ferromagnetic films were investigated using modified second order Heisenberg Hamiltonian. Several easy and hard directions could be observed in many 3-D plots. Angle between easy and hard directions was close to 107 degrees in this range of thickness. The energy required to rotate spins from easy to hard direction in ferromagnetic films gradually increases with the number of spin layers. The magnetic easy direction of ferromagnetic films gradually rotates from the perpendicular direction to the in plane direction, as the number of spin layers is increased. This implies that a preferred in plane orientation can be observed at higher thicknesses. Our theoretical results agree with the experimental data of ferromagnetic thin films. Although the data of easy and hard directions given table 1 were

calculated using graphs of $\frac{E(\theta)}{\omega}$ versus angle for

$\frac{J}{\omega} = \frac{D_m^{(4)}}{\omega} = \frac{K_s}{\omega} = \frac{N_d}{\mu_o \omega} = \frac{H_{in}}{\omega} = \frac{H_{out}}{\omega} = \frac{D_m^{(2)}}{\omega} 10$, the same simulation can be carried out for

other values of these magnetic energy parameters as well. The easy axis rotates from out of plane to in plane direction with the increase of thickness of ferromagnetic film, because demagnetization factor and dipole interaction dominates the magnetic anisotropies with the increase of thickness.

References:

1. Hucht A and Usadel K.D. (1997). Reorientation transition of ultrathin ferromagnetic films. *Physical Review B* **55**: 12309.
2. Hucht A and Usadel K.D. (1999). Theory of the spin reorientation transition of ultra-thin ferromagnetic films. *Journal of Magnetism and Magnetic materials* **203(1)**: 88-90.
3. Usadel K.D and Hucht A. (2002). Anisotropy of ultrathin ferromagnetic films and the spin reorientation transition. *Physical Review B* **66**: 024419.
4. Nowak U. (1995). Magnetisation reversal and domain structure in thin magnetic films: Theory and computer simulation. *IEEE transaction on magnetics* **31(6-2)**: 4169-4171.
5. Dantziger M, Glinsmann B, Scheffler S, Zimmermann B and Jensen P.J. (2002). In-plane dipole coupling anisotropy of a square ferromagnetic Heisenberg monolayer. *Physical Review B* **66**: 094416.
6. Tsai Shan-Ho, Landau D.P and Schulthess Thomas C. (2003). Effect of interfacial coupling on the magnetic ordering in ferro-antiferromagnetic bilayers. *Journal of Applied Physics* **93(10)**: 8612-8614.
7. Radomska Anna and Balcerzak Tadeusz (2003). Theoretical studies of model thin EuTe films with surface elastic stresses. *Central European Journal of Physics* **1(1)**: 100-117.
8. Cates James C. and Alexander Jr Chester. (1994). Theoretical study of magnetostriction in FeTaN thin films. *Journal of Applied Physics* **75**: 6754-6756.
9. Ernst A, Lueders M, Temmerman W.M, Szotek Z and Van der Laan G. (2000). Theoretical study of magnetic layers of nickel on copper; dead or live?. *Journal of Physics: Condensed*

matter **12(26)**: 5599-5606.

10. Kovachev St and Wesselinowa J.M. (2009). Theoretical study of multiferroic thin films based on a microscopic model. *Journal of Physics: Condensed matter* **21(22)**: 225007.
11. Zhao D, Feng Liu, Huber D.L and Lagally M.G. (2002). Step-induced magnetic-hysteresis anisotropy in ferromagnetic thin films. *Journal of Applied Physics* **91(5)**: 3150-3153.
12. Spisak D and Hafner J. (2005). Theoretical study of FeCo/W(110) surface alloys. *Journal of Magnetism and Magnetic Materials* **286**: 386-389.
13. Samarasekara P. (2003). A Pulsed RF Sputtering Method for Obtaining Higher Deposition Rates. *Chinese Journal of Physics* **41(1)**: 70-74.
14. Samarasekara P. (2002). Easy Axis Oriented Lithium Mixed Ferrite Films Deposited by the PLD Method. *Chinese Journal of Physics* **40(6)**: 631-636.
15. Samarasekara P. (2006). Second order perturbation of Heisenberg Hamiltonian for non-oriented ultra-thin ferromagnetic films. *Electronic Journal of Theoretical Physics* **3(11)**: 71-83.
16. Samarasekara P. (2006). A solution of the Heisenberg Hamiltonian for oriented thick ferromagnetic films. *Chinese Journal of Physics* **44(5)**: 377-386.
17. Samarasekara P. (2011). Investigation of Third Order Perturbed Heisenberg Hamiltonian of Thick Spinel Ferrite Films. *Inventi Rapid: Algorithm Journal* **2(1)**: 1-3.
18. Samarasekara P and William A. Mendoza. (2011). Third Order Perturbed Heisenberg Hamiltonian of Spinel Ferrite Ultra-thin films. *Georgian electronic scientific journals: Physics* **1(5)**: 15-24.

19. Samarasekara P. (2010). Determination of energy of thick spinel ferrite films using Heisenberg Hamiltonian with second order perturbation. *Georgian electronic scientific journals: Physics* **1(3)**: 46-49.
20. Samarasekara P and Saparamadu Udara (2013). Easy axis orientation of barium hexa-ferrite films as explained by spin reorientation. *Georgian electronic scientific journals: Physics* **1(9)**: 10-15.
21. Samarasekara P and William A. Mendoza (2010). Effect of third order perturbation on Heisenberg Hamiltonian for non-oriented ultra-thin ferromagnetic films. *Electronic Journal of Theoretical Physics* **7(24)**: 197-210.
22. Samarasekara P., Abeyratne M.K. and Dehipawalage S. (2009). Heisenberg Hamiltonian with Second Order Perturbation for Spinel Ferrite Thin Films. *Electronic Journal of Theoretical Physics* **6(20)**: 345-356.
23. Samarasekara P and Saparamadu Udara (2012). Investigation of Spin Reorientation in Nickel Ferrite Films. *Georgian electronic scientific journals: Physics* **1(7)**: 15-20.
24. Parlak U., Akoz M.E., Tokdemir Ozturk S. and Erkovan M. (2015). Thickness dependent magnetic properties of polycrystalline nickel thin films. *Acta Physica Polonica A* **127(4)**: 995-997.
25. Araya-Pochet J., Ballentine C.A. and Erskine J.L. (1988). Thickness and temperature dependent spin anisotropy of ultrathin epitaxial Fe films on Ag(100). *Physical Review B* **38(11)**: 7846-7849.